Progress In Electromagnetics Research C, Vol. 57, 193–203, 2015

Design of Offset Dual-Reflector Antennas for Improving Isolation Level between Transmitter and Receiver Antennas

Ki-Bok Kong[1], Hee-Su Kim[1], Rao Shahid Aziz[2, *], and Seong-Ook Park[2]

Abstract—This paper presents the improved isolation property of the signals among transmitter and receiver antennas. The separation wall is laid at the center of the antennas to improve the isolation level between them. The introduced separation wall has serrated edges mounted on three sides, i.e., top, left and right sides. These mounted serrated edges are implemented to reduce the diffraction which may occur due to the linear edge of the wall. The Fresnel diffraction problem has been solved using analytical method in order to get the optimized structure of the serration. The Fresnel diffraction patterns due to different sizes of the serration are obtained, and their relative powers are compared to each other. The implemented antenna system with the serration wall is composed of corrugated feed horn, orthogonal mode transducer, and offset dual-reflector parabolic antennas. The effect of serration is well demonstrated by the measurement of isolation level of the antenna system. The measured results show that the serrated edges enhanced the isolation property among transmitter and receiver antennas.

1. INTRODUCTION

The rapid expansion of vertical offset-fed (or offset) parabolic antenna in cloud, rain and weather radars is due to the advantages of its suppressed sidelobe level, higher aperture efficiency and the geometrical structure which the water does not collect into [1, 2]. The antenna system that has separated transmitter and receiver antennas has good isolation level, and the separation wall between the two antennas further improves this level. But if the edges of separation walls are of shape of straight or linear, then the diffraction of edge occurs, which affects the received signal pattern and degrades the isolation level between transmitter and receiver antennas. However, to reduce the effect caused by the diffraction of linear edge, serrated edge can be a good candidate on the separation wall. Serrated structure is widely used to the edge of reflector in CATR (Compact Antenna Test Range) system to reduce the effect of the diffraction [3–5]. Moreover, serrated edge is used to the edge of reflector antenna to improve the magnetic field pattern [6]. The antenna for the rain radar system needs to have low cross polarization level in order to utilize in dual polarized signal. But it is well known that the offset antenna generates a cross-polarization introduced by the offset geometry [7]. To cancel the cross polarization in offset reflector antenna, corrugated feed horn was introduced [8].

In this paper, we have introduced a separation wall with serrated edges to improve the isolation property of the signals among transmitter and receiver antennas. The separation wall having the serrated edge is applied to alleviate the effect of the diffraction on the edges. The optimized serration structure was obtained using the Fresnel integral formula. Furthermore, in order to minimize the cross polarization of offset antenna, we used the circular corrugated feed horn. The orthogonal mode transducer was combined with this corrugated feed horn to generate dual polarized signal. The offset

Received 13 April 2015, Accepted 19 May 2015, Scheduled 18 June 2015

* Corresponding author: Rao Shahid Aziz (rshahid@kaist.ac.kr).

[1] Kukdong Telecom., Bujeok-Myun, Nonsan-City, Korea. [2] Microwave and Antenna Laboratory, Department of Electrical Engineering, Korea Advanced Institute of Science and Technology (KAIST), 291 Daehak-ro, Yuseong-gu, Daejeon 305-701, Republic of Korea.

parabolic curves is obtained by using the offset parabolic equation and hence utilized in the designing of offset reflector antenna. The designed antenna is simulated by the CST microwave studio simulation software. The fabricated antenna is presented, and its electrical characteristics are measured, i.e., gain, sidelobe level, beamwidth, isolation level at the far and near-field measurement system. Also the measured results are compared to the simulated ones, which show reasonable agreement. The isolation level of the serrated edge of wall is estimated and compared to the rectangular edge of wall. The radiation pattern is obtained by far-field outdoor test and confirms the effect of the serration.

2. ANTENNA SYSTEM DESIGN AND PROTOTYPES

2.1. Design of Corrugated Feed Horn and OMT (Orthogonal Mode Transducer)

Figure 1 shows the complete designed overview of the K-band offset dual-reflector antennas of the rain radar antenna system. It can be seen that the transmitter and receiver antennas are separated by the rectangular wall having antenna radome at the front and back side. There is a space inside separation wall in which the electrical components for producing and receiving K-band radio frequency signal are installed.

The primary source, located at the focal point, is the corrugated circular horn. The horn parameters are optimized to achieve the desired performance in terms of low cross-polarization. The proposed corrugated feed horn diagram is shown in Figure 2. The presented corrugated horn has been designed and simulated using commercially available CST software and TICRA's horn design software. The fundamental mode of the input waveguide is TE_{11} mode, and mode converter of the horn provides a smooth transition from TE_{11} to HE_{11}. The total number of corrugations is 20 including the mode convert, and the length is 3.54λ, where λ is the operating wavelength.

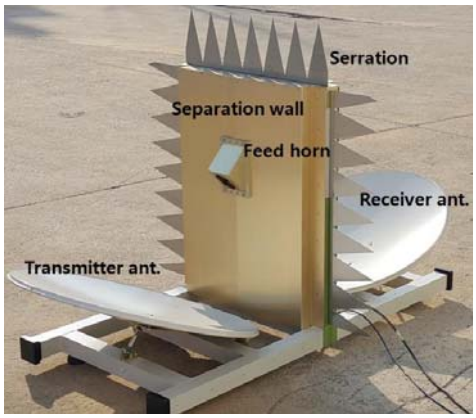

Figure 1. View of the offset dual-reflector antennas.

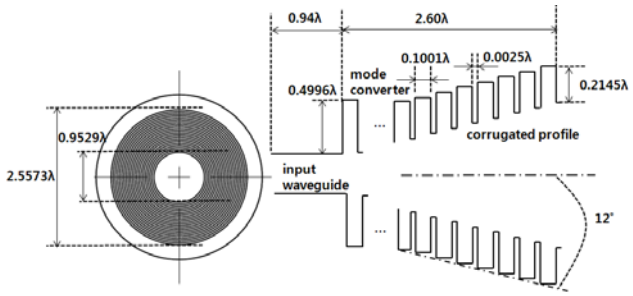

Figure 2. Geometry of circular corrugated feed horn.

Figure 3 shows the directive gain which is about 16 dBi and the radiation pattern of H-plane (azimuth) and V-plane (elevation). It can be observed that both the planes are symmetrical and that the difference of magnitudes is less than 0.2 dBi in $\pm 30^\circ$ which is the tapered angle of 12°. As reported in [9], 11 to 12 dB is commonly used as the edge taper considering the spill over and the under-illumination of the aperture.

The orthogonal mode transducer (OMT) is used to separate the linearly polarized signal into vertical and horizontal polarizations. The dimension of OMT is optimized to achieve the required field distribution using CST simulation software. Figure 4 describes that OMT has two TE_{10} mode ports going through vertically and horizontally polarized signal, and one TE_{11} mode port connecting to the circular waveguide port of the corrugated horn. As a result of measurement at K-band frequency, in the condition of combining corrugated horn with OMT, the obtained insertion loss (S_{32}) is less than -38 dB. The measurement results are described in experimental results and discussion section.

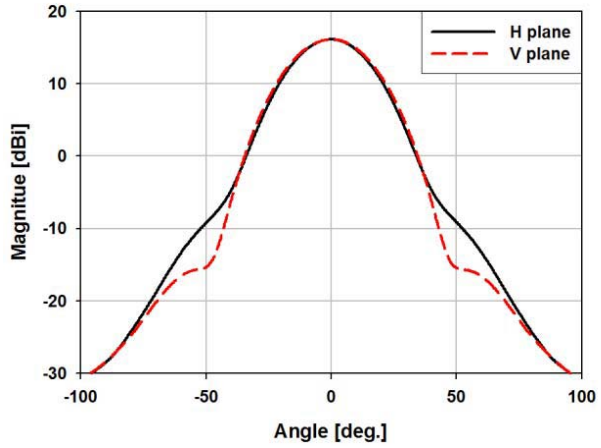

Figure 3. Simulated radiation pattern of corrugated feed horn using CST.

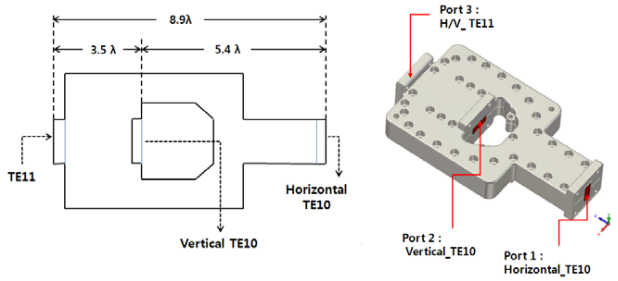

Figure 4. Geometry of OMT describing the ports.

2.2. Design of Dual-Reflector Parabolic Antenna

The 3D curve of the offset parabolic reflector can be calculated by the parabolic equation [10]. We have assumed that the elliptical rim of the reflector lies on xy-plane and at the center. The major axis of the rim is along the x-axis, and on the other hand, the minor axis is along the y-axis. The depth function $d(x, y)$ of offset reflector is defined by the following expression [11]:

$$d(x,y)=\frac{2fL^3}{D\left(L^2-D^2\right)}\left\{\left[1+\frac{xD^2\sqrt{L^2-D^2}}{fL^3}+\frac{D^2\sqrt{L^2-D^2}}{4f^2L^4}\left(\frac{D^2}{4}-y^2\right)\right]^{1/2}-1-\frac{xD^2\sqrt{L^2-D^2}}{2fL^3}\right\} \quad (1)$$

where,

L = major axis length;
D = diameter of aperture;
f = focal length.

The focal length to diameter ratio f/D is determined as 0.625 which is optimized considering the tapered angle of horn and the available space for antenna structure. If the parallel distance from feed horn to

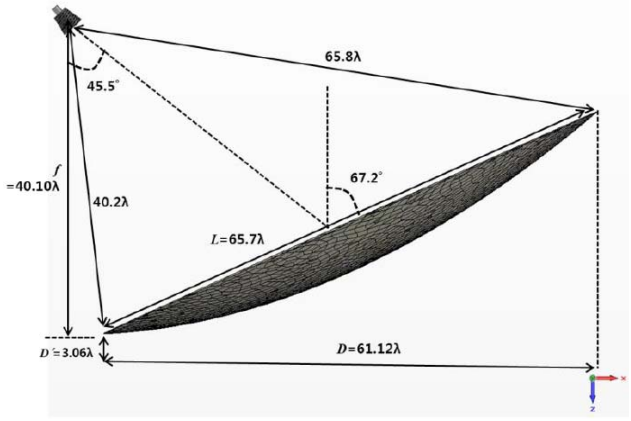

Figure 5. Parameters of offset parabolic antenna depicted by CST.

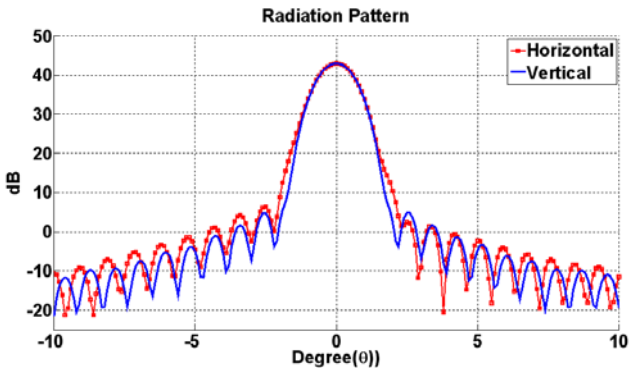

Figure 6. Simulated far-field radiation pattern of parabolic antenna using CST.

lowest rim of parabolic antenna is chosen to be $D' = 3.06\lambda$ considering feed horn size and feed blockage then the offset angle can be obtained from equation $(90 - \tan^{-1}\{\frac{4f}{2D'+D}\})$, and it becomes 22.8° [11]. Figure 5 illustrates the geometry configuration of designed offset parabolic antenna and describes its respective parameters.

We have obtained the 3D coordinate points of reflector from Equation (1). The 3D parabolic surface can be made by CATIA (Computer Aided Three-dimensional Interactive Application) that is a multi-platform CAD/CAM/CAE commercial software. On the other hand, by using CST, we have simulated the single offset parabolic antenna illuminated by the far-field source of horn. The radiation pattern of the single offset parabolic antenna is shown in Figure 6. From the simulation it is observed that the half-power bandwidth (HPBW) of the single offset parabolic antenna is 1.2°; the directivity gain is 43 dB; the sidelobe level is better than 28 dB.

2.3. Design of the Serrated Wall

The separation wall faces the problem of diffraction due to linear or straight edges. In order to overcome this deficiency, serrated edge is mounted on the three sides of separation wall, i.e., top, left and right. The material of the serration wall is aluminum, and the serrated structure is made by stainless steel. The separation wall with serrated edge is located at Fresnel field viewing from parabolic antenna. Therefore, the effect of serration is investigated by the Fresnel diffraction pattern which represents the electrical field illuminated by serrated wall. As reported in [3], Fresnel diffraction pattern due to a rectangular aperture with serrated edge can be calculated by Fresnel integral formula. In order to apply the Fresnel integral to the diffraction effect problem, the integral region can be divided into three parts as depicted in Figure 7. The whole integral region of the separation wall can be obtained by subtracting the sum of region 1 and region 2 from region 3.

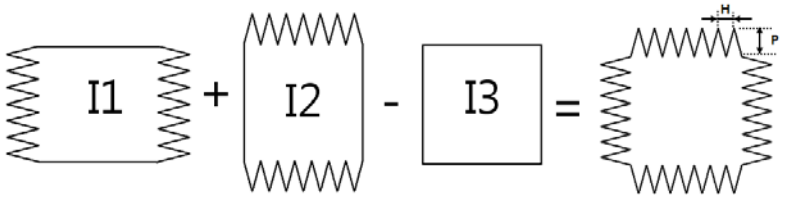

Figure 7. Geometry of serrated edge wall.

Therefore, the field function at observation point (x, y, z) can be expressed as

$$E(x, y, z) = \frac{j\sqrt{\pi}E_0}{2} e^{-jkz} (I_1 + I_2 - I_3) \tag{2}$$

where, E_0 is an initial constant value at $(x, y, 0)$, and k is a propagation constant.

I_1 is an integral formula at region 1 and given by,

$$I_1 = \int_{c(y-b_0)}^{c(y+b_0)} \left(F\left(cx - cg^{-}(y - v/c)\right) - F\left(cx - cg^{+}(y - v/c)\right)\right) e^{-j\pi v^2/2} dv \tag{3}$$

where, $g+$ and $g-$ are the functions defined on the boundary describing the serrated edges of region 1, and F is the Fresnel integral formula and $c = \sqrt{(2/\lambda z)}$. On the other hand, the integral formulas for I_2 and I_3 are similarly expressed as the variables are symmetrical. Whereas, F is expressed by the following integral formula,

$$F(x) = \int_0^x \frac{e^{-jt}}{\sqrt{2\pi t}} dt \tag{4}$$

The Fresnel integral can be calculated by approximate method and can be written as,

$$\begin{aligned} &\text{For } 0 \le x \le 4 \quad F(x) = e^{-jt}\sqrt{\frac{x}{4}}\sum_{n=0}^{11}(a_n + jb_n)\left(\frac{x}{4}\right)^n \\ &\text{For } x \ge 4 \quad F(x) = \frac{1-j}{2}e^{-jt}\sqrt{\frac{4}{x}}\sum_{n=0}^{11}(c_n + jd_n)\left(\frac{4}{x}\right)^n \end{aligned} \tag{5}$$

where the constants a_n, b_n, c_n, and d_n are reported in [12].

Figure 8 illustrates the geometry for calculating the field pattern of serrated edges. In order to get the optimized serrated edges for suppressing the effect of diffraction, we have calculated the field pattern along x-axis fixing $y = 0$ and $z = 48\lambda$ by using Equation (2) considering that the plane wave is in the direction along z-axis. At first fixing the value of H observed in Figure 7, field pattern has been calculated by varying the value of P, and the results are displayed in Figure 9. It can be observed in Figure 9 that the influence of serrated edges is different by changing the size of P. Moreover, when the value of P is 15λ the maximum magnitude of pattern is near 0. Next fixing the P at 15λ, Fresnel diffraction pattern is calculated by varying the value of H. It is noticed that when H is 8λ, the maximum magnitude of pattern is near 0 as shown in Figure 10. According to the analysis result, the design of serrated edge of separation wall is optimized at $H = 8\lambda$ and $P = 15\lambda$.

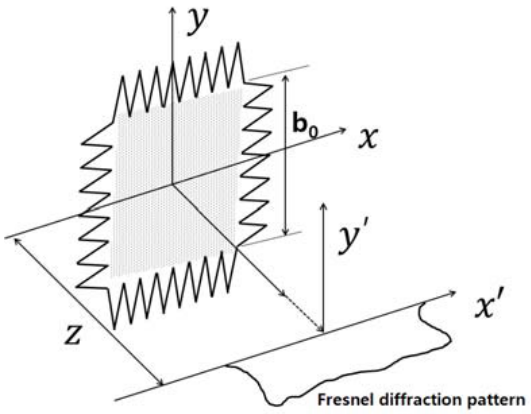

Figure 8. Geometry about diffraction effect for aperture structure with serration.

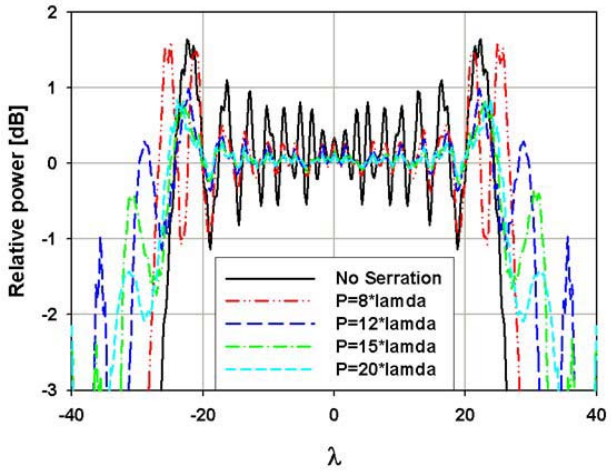

Figure 9. Fresnel diffraction pattern along x-axis when fixing $y = 0$ and $z = 48\lambda$.

3. EXPERIMENTAL RESULTS AND DISCUSSIONS

3.1. Measurement of Corrugated Horn combining with OMT (Orthogonal Mode Transducer)

Figure 11 shows the complete overview of designed corrugated feed horn combined with OMT (Orthogonal Mode Transducer). The measured insertion loss characteristic of vertical and horizontal ports is plotted in Figure 12. As a result of measurement, the insertion loss of ports is less than 1 dB. Moreover, measured port-to-port isolation between vertical and horizontal ports is shown in Figure 13. The isolation between the two ports is less than -40 dB. The characteristic of the insertion loss and isolation of corrugated feed horn agreed well with designed intention.

The radiation pattern of the corrugated horn is obtained from the far-field measurement of corrugated horn and depicted in Figure 14. It can be noticed that the difference between the

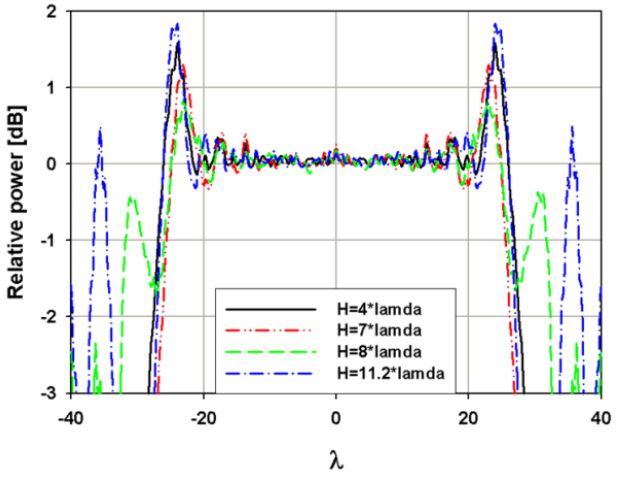

Figure 10. Fresnel diffraction pattern along x-axis when fixing $P = 15\lambda$.

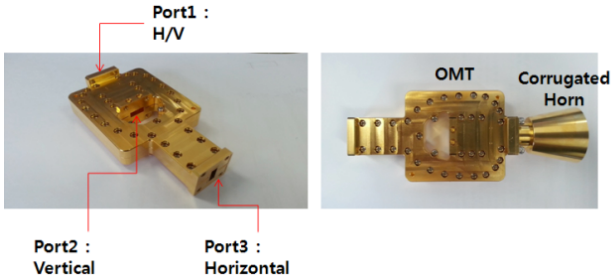

Figure 11. View of the corrugated horn combined with OMT.

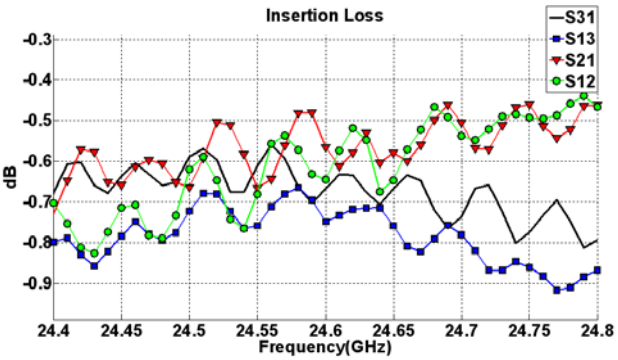

Figure 12. Insertion loss of the corrugated horn with OMT tested by network analyzer.

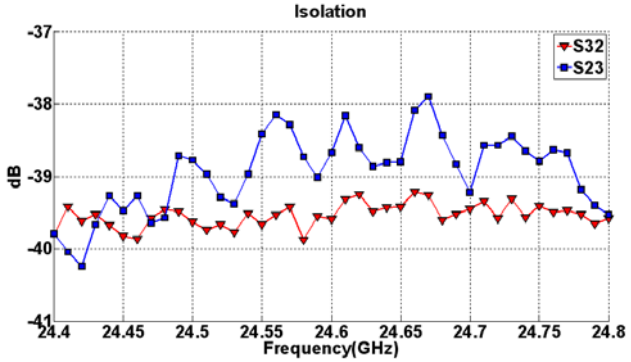

Figure 13. Port-to-port isolation of the corrugated feed horn with OMT tested by network analyzer.

measurement and simulation parallel patterns in the region of $\pm 30^\circ$ is less than 0.1 dB. In addition to that it is evident in Figure 14 that the cross-polarization level is 30 dB higher than co-polarization pattern.

3.2. Measurement of Offset Parabolic Antenna

Figure 15 shows the measured antenna patterns of offset parabolic antenna at the center frequency 24.6 GHz. The directivity gains of parallel polarized patterns are 42 dB. HPBW of the horizontally parallel polarized pattern is 1.2° and coincides with the vertically parallel polarized pattern. The cross polarization level in vertical polarization is 28 dB, whereas, in horizontal polarization it is about 23 dB. The measurements were carried out at the near-field measurement system with the capability of 40 GHz measurement.

3.3. Measurement of Isolation between Transmitter and Receiver Antennas

The isolation level between transmitter and receiver antennas can be obtained by measuring S_{21} parameter. Reported corrugated horn is combined with OMT in Figures 4 and 11, and S_{21} measurement can be performed after choosing the input and output ports of transmitter and receiver feed horns of

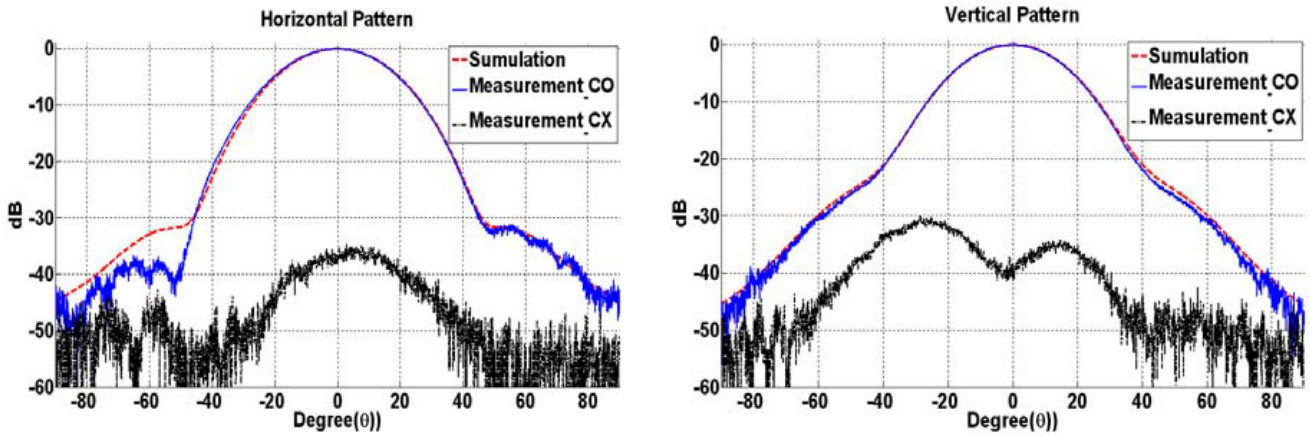

Figure 14. The normalized radiation pattern with horizontal and vertical polarization of corrugated feed horn for observing the cross polarization.

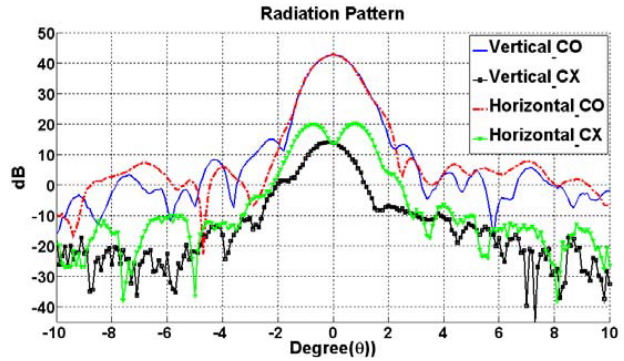

Figure 15. The measured radiation patterns with horizontal and vertical polarization of the offset parabolic antenna measured at the near-field measurement system.

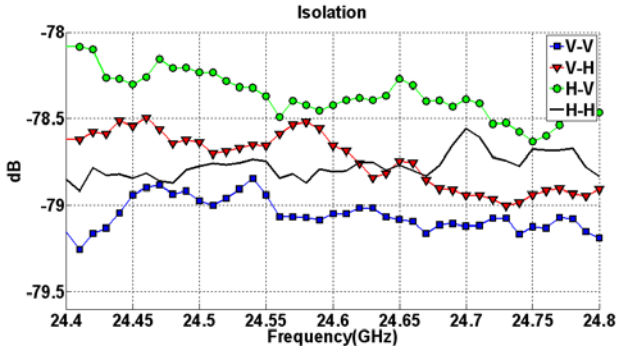

Figure 16. S_{21} parameter of horizontal or vertical polarization transmitter and receiver antennas at the outdoor tested by network analyzer.

Figure 17. View of the separation wall with rectangular structure.

the vertical port. The horizontal and vertical polarization ports are used as input and output ports alternately. The measurement of the isolation level is carried out at the outdoor place which is the same as the actual rainfall measurement environment. The four linear polarization combinations, i.e., V-V, V-H, H-V, and V-V are used for the measurement of isolation level, where, V and H represent

the vertical and horizontal polarizations. Similarly, T-R combination represents the polarization of transmitter port T and the polarization of receiver port R. T and R represent vertical and horizontal linear polarizations, respectively, so the four combinations of V-V, V-H, H-V, and V-V can be possible. These are concerned with the scattering matrix whose components are related to the scattering field of the water drop. The measurements about the four polarization combinations (V-V, V-H, H-V, and V-V) were performed 20 times and considered an average on values of the sum. Figure 16 shows the S_{21} parameter of horizontal or vertical polarization transmitter and receiver antennas at the outdoor. It can be noticed that the antenna-to-antenna isolation level is less than 78 dB.

Next in order to observe the effect of serrated edges up pressing the effect of the diffraction, we have measured S_{21} parameter in an environment in which the signal is reflected only from the upward direction at close range. The antenna is surrounded by the absorbers. Three cases have been performed for the measurement of isolation level. The first case is the separation wall with the serrated edge.

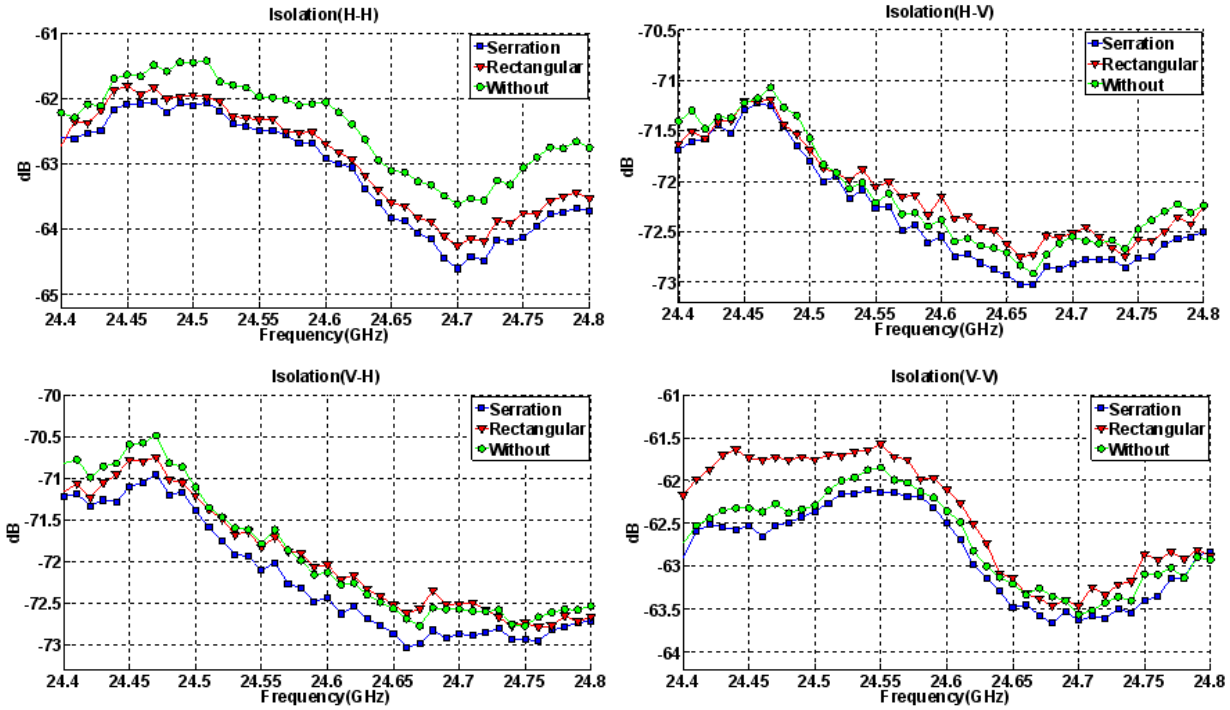

Figure 18. S_{21} parameter value in three different cases for H-H, H-V, V-H, V-V polarization combinations in the room with only upwind reflected signal tested by network analyzer.

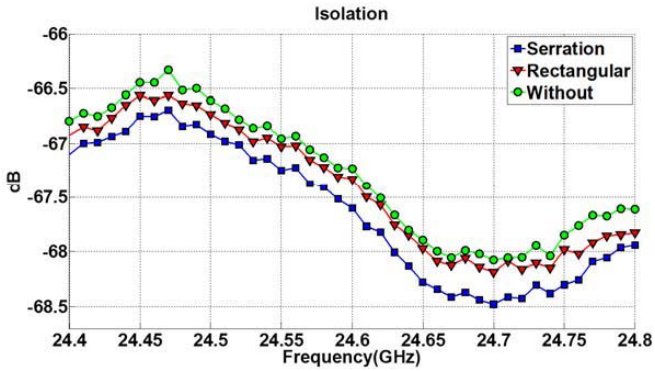

Figure 19. S_{21} parameter value in three different cases after summing and averaging in the room with only upwind reflected signal tested by network analyzer.

The second case is the separation wall with the rectangular structure which has the same area as the serration edges as shown in Figure 17, and the third case is the separation wall without the serrated edge and the rectangular structure.

The measurement of S_{21} parameter was performed 20 times with the four combinations of H-H, H-V, V-H, V-V polarization. After summing the value of each polarization case, the sum is divided by 20. Figure 18 shows the obtained measured results. The comparison can be made from the obtained plots that the isolation level of serrated wall with other cases has the best isolation level for each case of T-R polarization. Now these obtained values of the isolation level of H-H through V-V are summed, and the sum is averaged. This was a meaningful job because the fulfillment of rain fall measurement using rain radar has one cycle composed of H-H, H-V, V-H, and V-V. As shown in Figure 19, the isolation level of the serrated wall is evenly higher than other cases over all the frequencies.

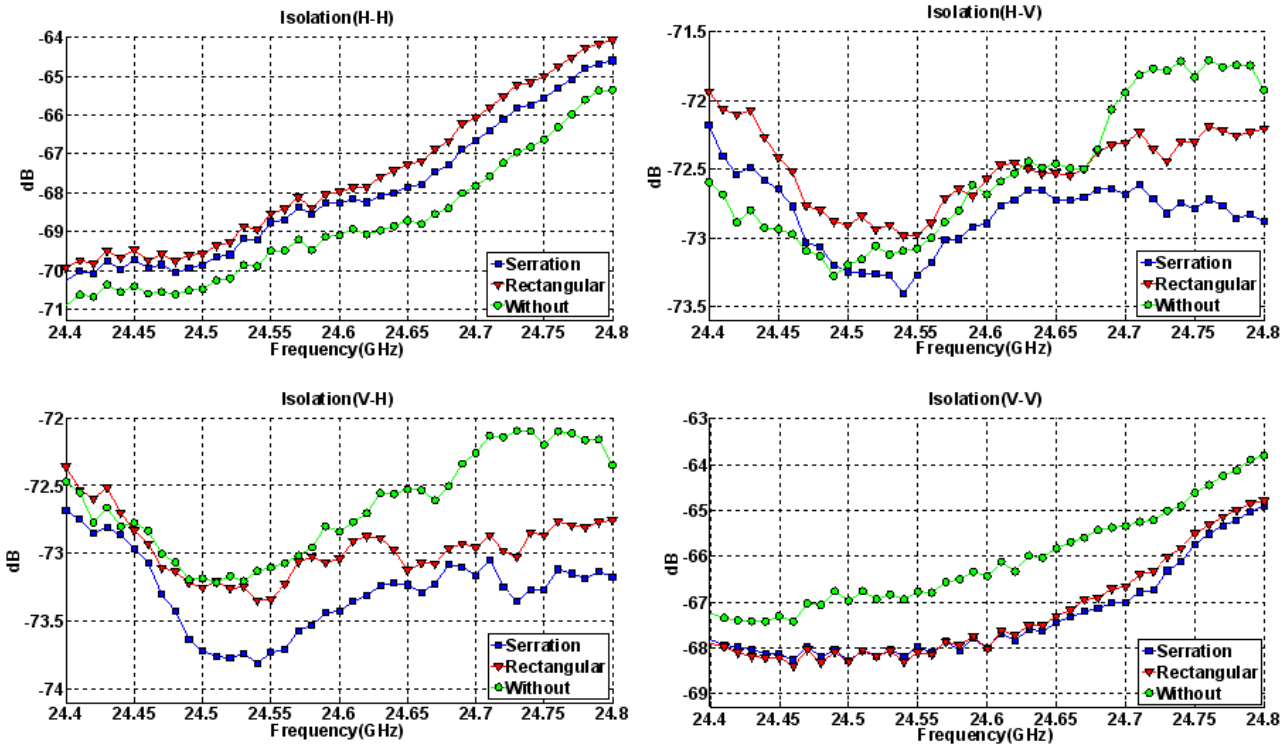

Figure 20. S_{21} parameter value in three different cases for H-H, H-V, V-H, V-V polarization combinations at the indoor room tested by network analyzer.

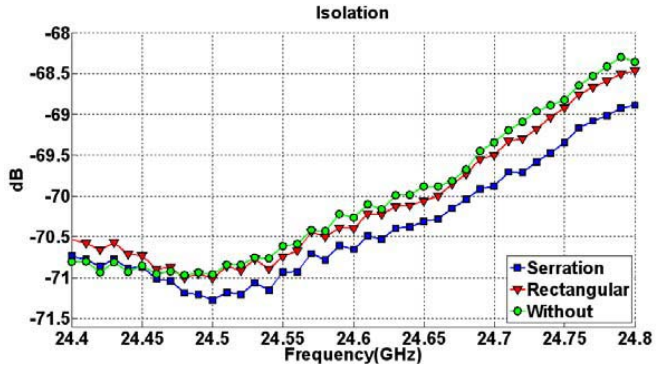

Figure 21. S_{21} parameter value in three different cases after summing and averaging at the indoor room tested by network analyzer.

Finally in order to observe the effect of serration in the environment of occurring the diffuse reflection, we have measured the isolation level at the indoor room that is blocked with wall. We have measured this scenario in the same manner as discussed above. Figure 20 shows the isolation level of the isolation wall in the three cases. In this measurement, both separation wall without serrated edge and separation wall with rectangular structure show better performance than the separation wall with serrated edges. However, it is shown from Figure 21 that if summing and averaging the obtained results, the isolation level of serrated wall is almost higher than others. It can be concluded that in the point of view of whole directional signal, the serration has the effect of enhancing isolation level between receiver and transmitter antenna.

4. CONCLUSION

The antenna for the rain radar system requires high gain, low side-lobe level, narrow HPBW and good isolation level between transmitter and receiver antennas. In this study, we have presented a method for the improvement of isolation between transmitter and receiver antennas. A separation wall is introduced among the two antennas. The linear edges of the separation wall causes diffraction. Therefore, in order to suppress the effect of diffraction on the edge, the separation wall with serration edges is mounted on the three sides. The Fresnel integral formula has been utilized to obtain the optimized size of the serrated wall structure. Moreover, the offset parabolic antenna is also designed by using parabolic geometric equations. The overall designed antenna system is composed of corrugated feed horn, orthogonal mode transducer, offset parabolic antennas and separation wall with serration edge structure. The design antenna system is fabricated, and the antenna radiation patterns, insertion loss and port-to-port isolation between ports of OMT are measured. It is found that the measured results agreed well with simulated data. Moreover, in order to observe the effect of serration, the antenna-to-antenna isolation level between transmitter and receiver antennas was measured. Three cases have been investigated, i.e., one by attaching the serration structure on the separation wall and the isolation level was measured, second by attaching the rectangular structure and third without any structure. Finally all the obtained measured results are compared, and it is found that separation wall with serration edges is suitable for suppressing the effect of diffraction and enhancing the isolation level.

ACKNOWLEDGMENT

This work was supported by the Ministry of Education (MOE) and National Research Foundation of Korea (NRF) through the Human Resource Training Project for Regional Innovation (NRF-2013H1B8A2032190).

REFERENCES

1. Spitz, S., A. Prata, J. Harrel, R. Perez, and W. Veruttipong, "A 94 GHz spaceborne cloud profiling radar antenna system," *Aerospace Conference*, Vol. 2, 685–694, Big Sky, MT, Mar. 2001.
2. Lee, H. and Y.-H. Kim, "Weather radar network with pulse compression of arbitrary nonlinear waveforms: KA-band test-bed and initial observations," *Progress In Electromagnetics Research B*, Vol. 25, 75–92, 2010.
3. Beeckman, P. A. and M. S. Castaner, "Prediction of the Fresnel region field of a compact antenna test range with serrated edges," *Proc. of IEEE Processing*, Vol. 133, No. 2, 108–114, Apr. 1986.
4. McKay, J. P. and Y. Rahmat-Samii, "Quiet zone evaluation of serrated compact range reflectors," *Ant. and Propag. Society Inter. Symp.*, 7–11, May 1990.
5. Lee, T. H. and W. D. Burnside, "Performance trade-off between serrated edge and blended rolled edge compact range reflectors," *IEEE Trans. on Ant. Propag.*, Vol. 44, No. 1, 87–96, Jan. 1996.
6. Acevedo, A. M., M. S. Castaner, and J. L. Besada, "Efficient and accurate hybrid GO-spectral algorithm to design conformal serrated-edge reflectors operating as collimators in millimeter wave compact ranges," *Ant. Measurement Tech. Associat. Symp.*, Oct. 2010.

7. Rudge, A. W. and N. A. Adatia, "Offset-parabolic-reflector antenna: A review," *Proceedings of the IEEE*, Vol. 66, No. 12, 1592–1618, Dec. 1978.
8. Granet, C. and G. L. James, "Design of corrugated horns — A primer," *IEEE Antennas Propag. Mag.*, Vol. 47, No. 2, 76–84, Apr. 2005.
9. Lee, S.-W. and Y. R. Samii, "Simple formulas for designing an offset multibeam parabolic reflector," *IEEE Trans. on Ant. Propag.*, Vol. 29, No. 3, 472–478, May 1981.
10. Uhm, M., A. Shishlov, and K. Park, "Offset-paraboloid geometry: Relations for practical use," *IEEE Antennas Propag. Mag.*, 77–79, Aug. 1996.
11. Milligan, T. A., *Modern Antenna Book*, 399–405, A John Wiley & Sons, 2005.
12. Boersma, J., "Computation of fresnel integrals," *Math. Computation*, Vol. 14, 380, 1960.